ACS Sustainable Chemistry & Engineering

Research Article

pubs.acs.org/journal/ascecg

# Distillation and Isolation of Commodity Chemicals from Bio-Oil Made by Tail-Gas Reactive Pyrolysis

Yaseen Elkasabi,* Charles A. Mullen, and Akwasi A. Boateng

Eastern Regional Research Center, Agricultural Research Service, U.S. Department of Agriculture, 600 E. Mermaid Lane, Wyndmoor, Pennsylvania 19038, United States

Supporting Information

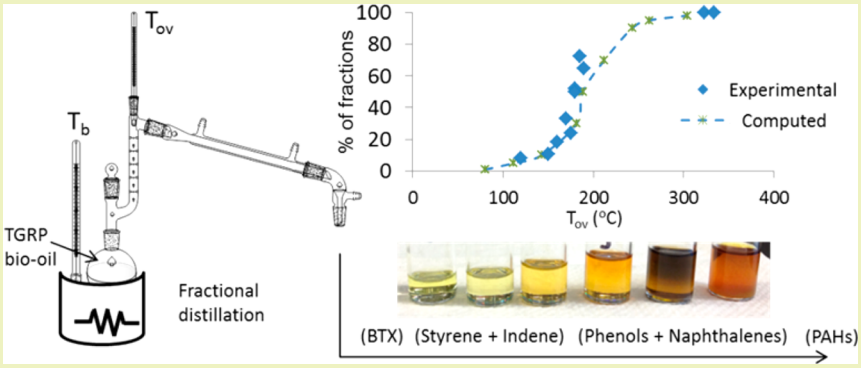


**ABSTRACT:** Owing to instabilities, very little has been accomplished with regard to simple cost-effective separations of fast pyrolysis bio-oil. However, recent developments in the use of tail-gas reactive pyrolysis (TGRP) (Mullen, C. A.; Boateng, A. A.; Goldberg, N. M. *Energy Fuels* **2013**.) provide higher quality bio-oils that are thermally stable. We used fractional distillation to isolate compounds from bio-oil produced by TGRP. All bio-oils produced from TGRP contained significantly less acid (0.2−4% total), trace amounts of aldehydes, and significantly higher concentrations of hydrocarbons and phenolics (5−20% each). One TGRP bio-oil rich in naphthalenes yielded the greatest mass of distillates (close to 65%). Using atmospheric distillation alone, we recovered the most distillates from another phenol-rich TGRP oil. Compared to traditional bio-oils, distillation of TGRP oils yielded three times more organic compounds; the yield improvement increases to a factor of 10 when the contribution of acetic acid is removed from consideration. Greater deficiencies in distillation yield occur with higher acids content (4 wt % acid). We categorized distillates according to boiling temperature and chemical components: benzene−toluene−xylenes (BTX), styrene, indene, pyridine, phenols, naphthalenes, acetic acid, and fluorene/anthracene. The relatively narrow product distributions allowed for the isolation of pure naphthalene by recrystallization from a naphthalene-rich fraction. Thermodynamic computation of the TGRP distillation profiles correctly predicted the experimental results, except when acid content equaled 4 wt %. The quality of the TGRP bio-oils allows for insertion into existing refineries, as well as the required Modeling and scale-up.

**KEYWORDS:** *Bio-oil, Upgrading, Pyrolysis, Distillation, Separations, Process modeling*

## INTRODUCTION

Biomass fast pyrolysis research aims to produce a renewable hydrocarbon feedstock for integration into a refinery infrastructure.[1] The drawbacks of biobased ethanol have increased the desire for drop-in biofuels, which are identical to those produced at the petroleum refinery. However, refiners have been reluctant to incorporate fast pyrolysis bio-oils because their chemical instabilities significantly harm equipment downstream from entry. If instabilities, corrosiveness, and particulates were decreased such that compatible and miscible blendstocks could be easily obtained from bio-oils, the time and cost savings associated with refinery integration could expedite fast pyrolysis as a long-term solution, as compared with other biofuel production options.[1,2] Perhaps the most abundant and critical process found in petroleum refineries is the distillation column. Every petroleum refinery introduces crude oil into a distillation tower, which separates petroleum into fractional cuts based on boiling temperature.[3] This separation allows for downstream upgrading and refining to occur at conditions appropriate for each fractional cut. Distillation is one of the oldest and most mature industrial chemical processes,[4] such that even small process improvements can significantly increase profits.[4−6] Because petroleum is naturally deoxygenated,[3] refineries have predominantly focused on post-distillation processes such as catalytic cracking and isomerizations,[3] hydrotreatment for removal of sulfur (HDS),[7] and removal of trace metals.[8] However, for fast pyrolysis bio-oils, the post-pyrolysis upgrading has focused entirely on hydrodeoxygena-

Received: May 1, 2014
Revised: June 10, 2014
Published: June 30, 2014

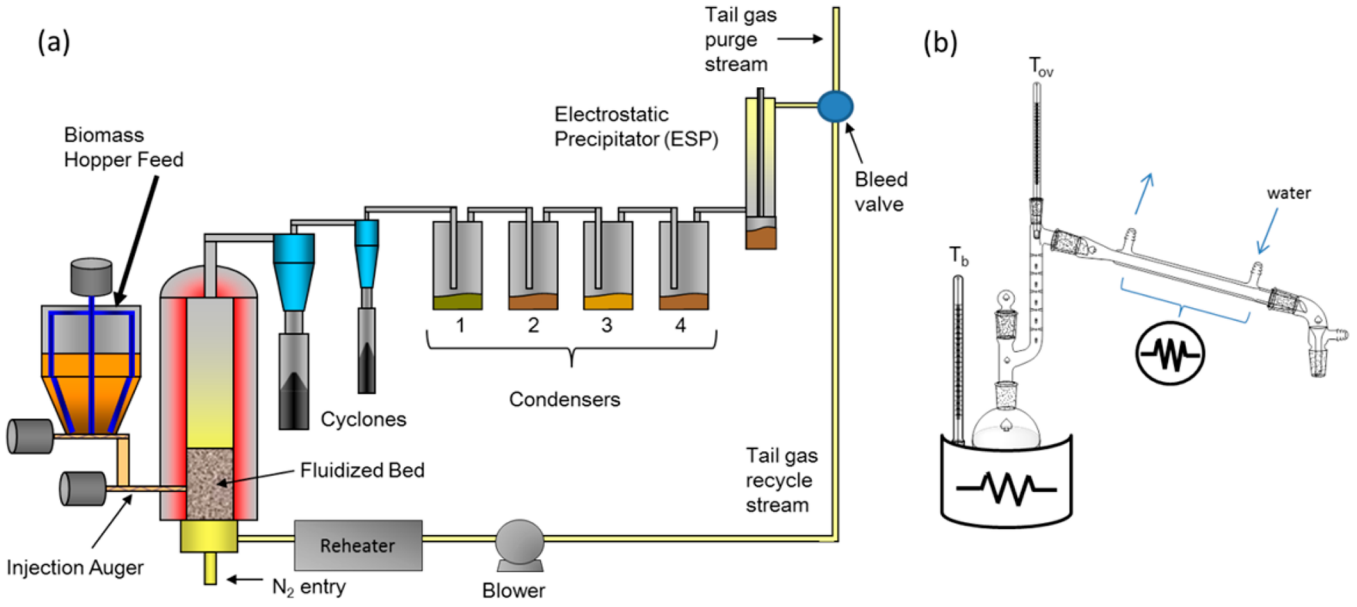


**Figure 1.** (a) Continuous fast pyrolysis process used to synthesize TGRP bio-oils. (b) Batch experimental setup used for the distillation of fast pyrolysis bio-oil. The temperatures of the bottoms heating mantle and the condenser were controlled externally, the latter utilizing either cooling water or heating tape.

tion (HDO)[9,10] of bio-oil before fractional distillation, instead of vice versa. That is because traditional bio-oil cannot distill as-is due to its unstable and highly reactive nature at even low temperatures (>50 °C). Mainly extraction-based techniques of separation have been investigated based on solvents like dichloromethane and water.[11,12]

Pyrolysis bio-oil production has matured relative to HDO because industrial-scale pyrolysis for fuels is closer to reality.[13,14] For HDO, many hindrances block successful pilot-scale validation,[15] let alone commercial production. These hindrances include but are not limited to copious consumption of nonrenewable hydrogen, high-pressure processing, and catalyst deactivation. Bio-oil separation processes could enhance hydrodeoxygenation (HDO) catalyst lifetimes due to removal of coke precursors. At the same time, valuable compounds and contaminants could be isolated and discarded, respectively. Because traditional atmospheric column distillation of bio-oil was more or less regarded as impossible, research into innovative and exotic bio-oil distillation techniques pressed forward. Investigations[16] and limited progress were made by using reactive and/or catalytic,[17,18] azeotropic,[19] and molecular[20,21] distillations, as well as internal recycling of distillate bottoms.[22]

Other than catalytic pyrolysis,[23] distillation of *in situ* deoxygenated bio-oil has yet to be investigated. In particular, a recent development at Agricultural Research Service uses tail-gas reactive pyrolysis (TGRP) to provide a reductive atmosphere during the pyrolysis step.[24] This reduction is accomplished by recycling a portion of the noncondensable gas byproducts back into the fluidized bed pyrolysis reactor. Depending on the overall processing conditions, TGRP results in 10 wt % bio-oil oxygen content or less. Acids, acetol, and furfurals in TGRP oil exist only in trace amounts, thus significantly eliminating undesired acidity and polymerization reactions. Valuable chemicals like phenols and naphthalenes exist in much greater concentrations in TGRP oil, which presents a viable alternative for replacing fossil fuel-derived petrochemicals. Thermal stability is greatly enhanced by the reduced acidity, increased aromatic hydrocarbons, and general reduction in oxygenated species. Every aforementioned characteristic makes TGRP bio-oil desirable and befitting for traditional distillation. Herein, we report high-yield and high-purity recoveries of TGRP bio-oil compounds via distillation. We also correlate computational models of distillation curves with experimental data.

## EXPERIMENTAL SECTION

**Fast Pyrolysis of Biomass.** Prior to fast pyrolysis experiments, all feedstocks were ground and dried. Switchgrass feedstock was provided by the McDonnell Farm (East Greenville, PA, U.S.A.), horse manure by the Equine Rehabilitation Center at Morrisville State College (Morrisville, NY, U.S.A.), and *Eucalyptus benthamii* by Embrapa Forestry (Candoi, Parana, Brazil). Fast pyrolysis of feedstock was carried out in the Eastern Regional Research Center (ERRC) fluidized bed fast pyrolysis system, as described previously.[24,25] Briefly, 2 kg/h of feedstock is fed through a fluidized sand bed reactor under 500 °C $N_2$ (Figure 1a). The resulting vapors then pass through a cyclone that separates out char particulates. Liquid phases are then condensed from the vapor by four condensers in series. A subsequent oil precipitates from the noncondensable gases (NCGs) by two electrostatic precipitators (ESPs) in series. All experiments used the oil obtained from the ESPs. For tail-gas recycle experiments, a fraction of the noncondensable gas stream was mixed with the $N_2$ stream and recycled into the fluidized bed, using a preheater and gas blower. The pyrolysis system recycled the tail-gas in the range of 50−70%, in that the reactive atmosphere consisted of 50−70% tail-gas with the balance being $N_2$.

**Distillation.** Bio-oils were distilled in a vacuum-jacketed Vigreux batch fractional distillation apparatus, equipped with a water coolant condenser and vacuum adapter outlet (Figure 1b). Prior to distillation, bio-oil samples were diluted with acetone in a 2:1 (vol:vol) excess, filtered via Büchner suction filtration (8 and 2 $\mu$m), and PTFE filtration (0.450 $\mu$m), and subsequently underwent rotary evaporation to remove the acetone. A total of 25g of filtered bio-oil was placed in a 100 mL round-bottomed flask and clamped to the distillation apparatus. A heating mantle heated the flask throughout the experiment, and glass wool insulated the flask. The flask was heated at ∼5−10 °C/min. Both the overhead vapor temperature ($T_{ov}$) and the distillation bottoms flask temperature ($T_b$) were recorded at the

Table 1. Chemical and Elemental Compositions of TGRP and Regular Pyrolysis Bio-Oils

| | TGRP | | | regular | | |
|---|---|---|---|---|---|---|
| | Type 1 | Type 2 | Type 3 | Type 1 | Type 2 | Type 3 |
| feedstock type (recycle rate) | manure (70%) | switchgrass (70%) | eucalyptus (50%) | manure (0%) | switchgrass (0%) | eucalyptus (0%) |
| wt % | | | | | | |
| BTX | 0.57 | 1.99 | 1.76 | 0.02 | 0.04 | 0.02 |
| phenols/cresols | 4.31 | 9.55 | 5.33 | 4.04 | 0.62 | 1.46 |
| pyridine | 0.48 | 0.16 | 0.00 | 0.00 | 0.00 | 0.00 |
| styrene | 1.87 | 2.10 | 1.03 | 0.00 | 0.00 | 0.00 |
| indene | 6.22 | 3.46 | 1.36 | 0.18 | 0.01 | 0.02 |
| fluorene/anthracene | 2.92 | 0.67 | 0.25 | 0.00 | 0.00 | 0.00 |
| naphthalenes | 16.83 | 6.41 | 2.38 | 0.34 | 0.04 | 0.04 |
| acetic acid/acetol | 0.23 | 0.81 | 3.97 | 8.04 | 6.87 | 10.39 |
| wt % (dry) | | | | | | |
| C | 79.53 | 80.29 | 67.93 | 67.35 | 53.81 | 59.45 |
| H | 5.75 | 5.67 | 6.00 | 6.82 | 5.36 | 5.99 |
| N | 3.54 | 1.50 | 0.37 | 2.31 | 0.52 | 0.13 |
| O | 11.18 | 12.54 | 25.70 | 23.52 | 33.21 | 34.43 |
| TAN (mg KOH/g) | 18 | 24 | 41 | 97 | 73 | 70 |
| moisture(wt %) | 2.08 | 3.08 | 2.63 | 7.31 | 7.98 | 6.90 |

end of each fraction collection (Figure 1b). When overhead temperatures exceeded 150 °C, the condenser water was shut off, and heating tape applied to the condenser was turned on. When the bottoms temperature reached 350 °C, vacuum was applied. After returning to room temperature and pressure, the bottoms product remaining in the flask was collected and pulverized with a mortar and pestle. Subsequent analysis was performed while accounting for phase separations. Distillate product yields were calculated based upon the original prefiltered bio-oil composition. Experiments were performed in duplicate.

**Naphthalene Recrystallization.** A minimal amount of hot methanol (solubility limit @ 55 °C = 0.41g/g solvent) was added to a vial containing a crude sample of recovered solids from distillation. After the solids completely dissolved, the vial was capped, left to cool at room temperature for 5 min, and then placed into a refrigerator for several hours. After recrystallization of naphthalene in the vial, the solid−solvent mixture was promptly decanted into a Büchner funnel and rinsed with cold methanol (0 °C). Naphthalene solids were then stored in a fresh vial and gently warmed in an oven to remove the remaining volatiles.

**Characterization and Analysis.** Elemental analysis (CHNS) was conducted via a Thermo EA1112 CHNS analyzer. Oxygen content was calculated by difference, and results were recalculated on a dry basis. Moisture content was measured with Karl Fischer titration in methanol with Hydranal Karl Fischer Composite 5 (Fluka) as the titrant. Total acid number (TAN) was measured using a Mettler T70 autotitrator using 0.1 M KOH in isopropanol as the titrant and wet ethanol as the titration solvent. Gas chromatography with mass spectroscopy (GC-MS) analysis of liquid products was performed on a Shimadzu GCMS QC-2010. The column used was a DB-1701, 60 m × 0.25 mm, 0.25 $\mu$m film thickness. The oven temperature was programmed to hold at 45 °C for 4 min, ramp at 3 °C/min to 280 °C, and hold at 280 °C for 20 min. The injector temperature was 250 °C, and the injector split ratio was set to 30:1. Helium carrier gas flowed at 1 mL/min. For GC-MS quantification of composition and yields, the "phenols/cresols" category included phenol, 2-methoxy-4-methylphenol, 2,4-dimethylphenol, 4-ethylphenol, 2,6-dimethoxyphenol, *o*-cresol, *m*-cresol, and *p*-cresol. The BTX category included benzene, toluene, *p*-xylene, and *o*-xylene. The naphthalenes category included naphthalene, 1-methyl-naphthalene, and 2-methyl-naphthalene.

**Theoretical Computation of Distillation Curves.** Theoretical distillation curves were generated using the distillation curve feature (true boiling points) in Pro-II process simulation software (Invensys, London, U.K.). Pro-II computed thermodynamic data using the Margules and/or non-random two-liquid (NRTL) activity models. Chemical compositional profiles, as measured by GC-MS, were used as base case inputs for computing distillation curves, while discounting the bottoms component.

## RESULTS AND DISCUSSION

**Pyrolysis Bio-Oil.** The experimental study investigated three types of TGRP bio-oil compositions. We examined a TGRP bio-oil relatively rich in bicyclic compounds (termed "Type 1", produced from horse manure feedstock), another rich in phenolics ("Type 2", produced from switchgrass), and a third with relatively elevated acids content ("Type 3", produced from *Eucalyptus benthamii*). The pyrolysis system (Figure 1a) produced bio-oil by either (1) normal fast pyrolysis, the product of which served as a control for baseline comparisons, or (2) TGRP. The organics dissolved in the condenser fractions comprise <5% of the total yield, while the ESP fraction contains low moisture (2−8 wt %) and contains the least amount of acid. For these reasons, we distilled only the ESP oil fractions. Types 1 and 2 TGRP were pyrolyzed at a 70% tail-gas recycle rate, which correlates with optimal quality TGRP bio-oil.[24] To investigate the effect of a reduced recycle rate on distillation efficiency, Type 3 TGRP was pyrolyzed at a 50% recycle rate (Tables S1 and S2, Supporting Information). Table 1 summarizes the characterization of bio-oils resulting from biomass pyrolysis from both TGRP and normal modes. Each bio-oil type possessed unique characteristics reflective of its overall chemical composition, with each type conducive to commodity chemical production. For instance, Type 1 bio-oil possessed very high concentrations of bicyclic and polyaromatic hydrocarbons (indene, naphthalenes, fluorene, and anthracene), which made for a very narrow product distribution. The GC-MS chromatogram appeared to show only a few large peaks, as opposed to the hundreds of small peaks normally present in bio-oil (Figure S1, Supporting Information). As a result, distillation of Type 1 resulted in fewer fractions that are distinct overall. Type 2 bio-oil contained the highest concentrations of phenolic compounds based upon measurements of specific phenol and cresol derivatives. This resulted in a slightly higher TAN value and moisture content. Type 3 bio-oil still contained a substantial acid content, as per the acetic


dx.doi.org/10.1021/sc5002879 | ACS Sustainable Chem. Eng. 2014, 2, 2042−2052

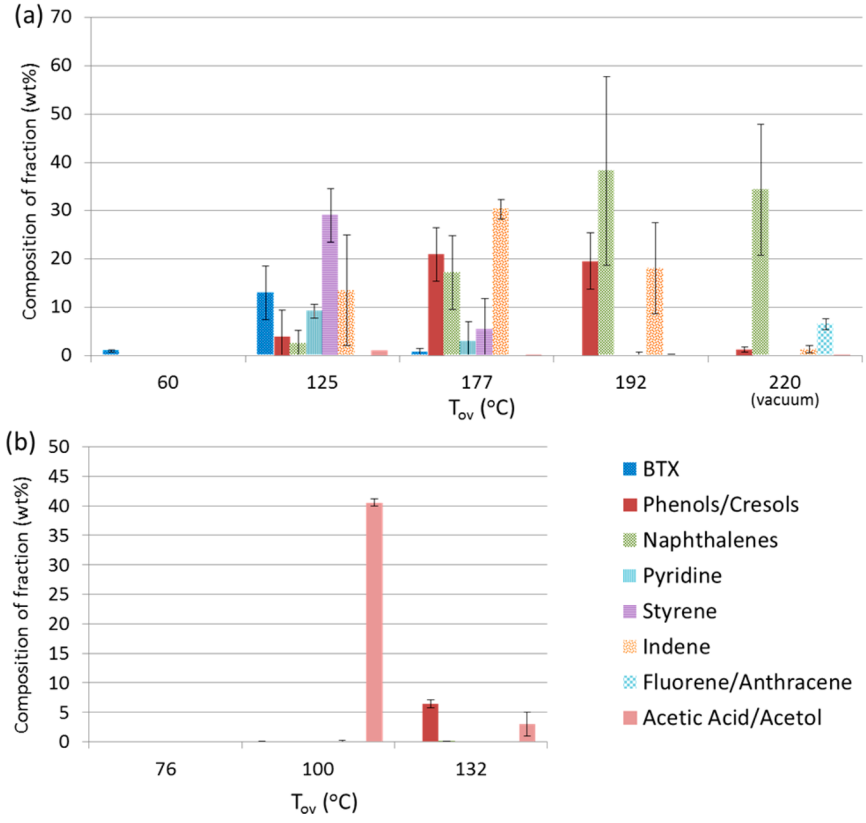


**Figure 2.** GC-MS compositions of each collected fraction from distillation of (a) TGRP and (b) regular bio-oil created with Type 1 biomass. Temperatures represent the final cut temperature. Error bars are one standard deviation.

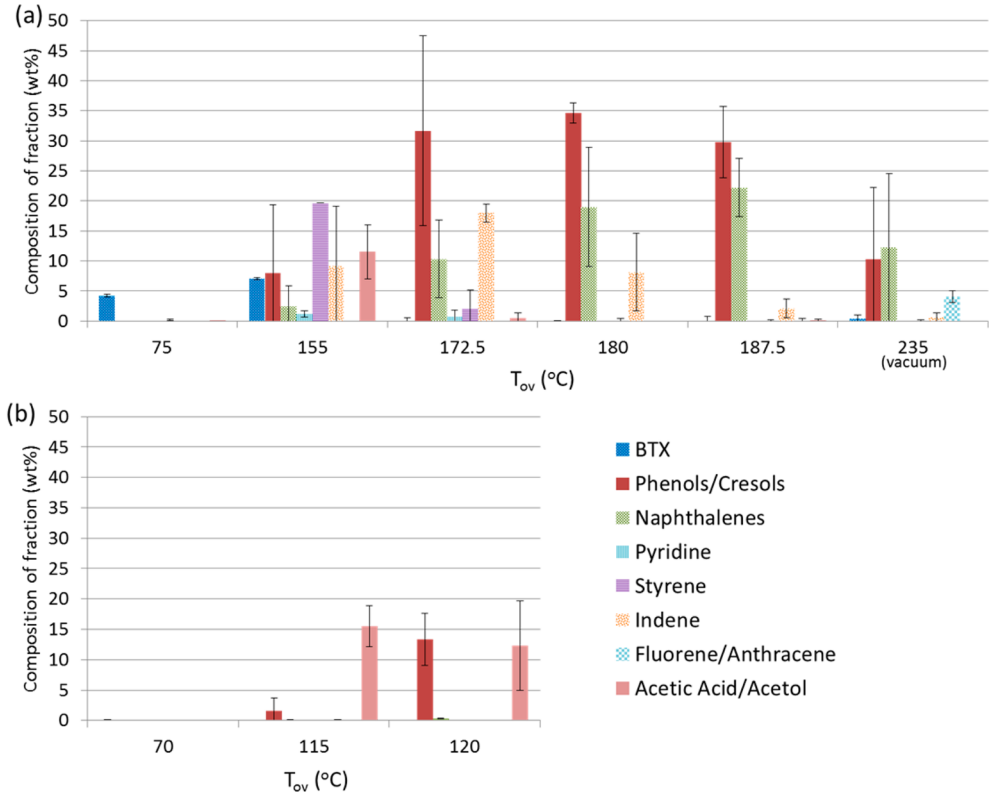


**Figure 3.** GC-MS compositions of each collected fraction from distillation of (a) TGRP and (b) regular bio-oils created with Type 2 biomass. Temperatures represent the final cut temperature.


dx.doi.org/10.1021/sc5002879 | *ACS Sustainable Chem. Eng.* 2014, 2, 2042−2052

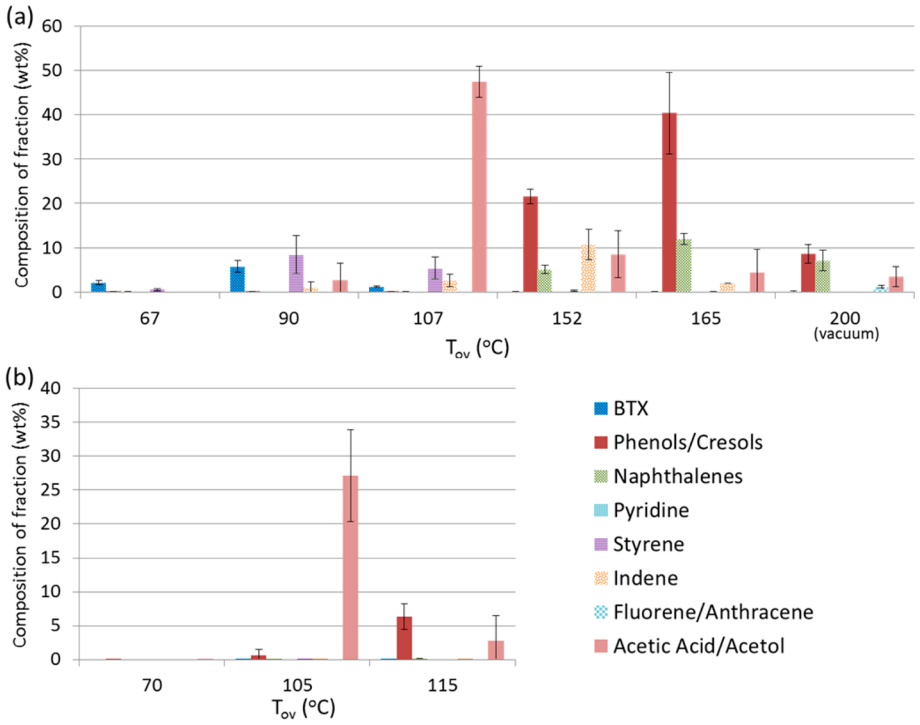


**Figure 4.** GC-MS compositions of each collected fraction from distillation of (a) TGRP and (b) regular bio-oils created with Type 3 biomass. Temperatures represent the final cut temperature.

acid concentrations and the TAN value, although its TAN value reduced significantly from that of regular bio-oil. The raised acid content is due to the less-than-optimal recycle ratio employed, and this shift plays a role in the subsequent experiments and analyses. While Type 3 TGRP oil has two variables changed from Types 1 and 2 (recycle rate and feedstock type), we have previously pyrolyzed the Type 3 feedstock at a slightly higher recycle rate of 60%.[26] Analysis of this 60% recycle rate bio-oil indicated that the composition (acid groups) was significantly lower than 50% recycling. 60% recycling of Type 3 TGRP produced oil compositions very similar to that of Type 2 bio-oil. These results indicated that the distillation of Type 3 oil at 50% differs primarily due to acid concentration.

As indicated by elemental analysis, all TGRP bio-oils contained significantly less oxygen, a key requirement for enhanced thermal stability. Regardless of processing conditions or biomass feedstock, nitrogen concentration increased significantly for TGRP bio-oils, indicating some incorporation of nitrogen into aromatic rings. Pyridine content reflects this elemental trend, but because pyridine accounts for a small portion of nitrogen, the rest must exist in higher molecular weight aromatics. For all TGRP bio-oils, moisture content decreased by more than half the original fraction found in regular bio-oil. As a result of the low TAN and oxygen content, the TGRP bio-oils possess thermal stability suitable for prolonged exposure to high temperatures.

**Fractional Distillation.** We filtered all bio-oil samples (>95% yield) in order to remove particulates that can catalyze polymerization and other unwanted side reactions. We used a batch distillation process for simplicity and reproducibility on a laboratory scale, as well as to avoid unpredictability when studying various feedstocks. As shown in Figure 1b, a heating mantle offered the most efficient means for temperature control to a high temperature. Heating tape affixed around the condenser provided a secondary source of temperature control in the event that high-boiling distillates condensed prematurely when either water coolant or ambient temperature was used. To assist with fractionation, the mantle heated the bottom flask in a gradual manner, and vapors passed through a Vigreux column. Collection of distillate fractions proceeded based upon the stability of $T_{ov}$. Each vial collected its corresponding fraction while $T_{ov}$ remained constant. Once $T_{ov}$ increased, the vial was switched to begin a new fraction. We used this procedure for two reasons: (1) Stable $T_{ov}$ values ensure accuracy for eventual thermodynamic and process modeling. (2) This procedure allows a particular chemical component to remain concentrated, as opposed to being scattered through multiple fractions. Due to the very volatile nature of light distillates within bio-oil, vacuum distillation was not employed until atmospheric distillation reached a maximum practical limit. Also, this procedure mimics current refinery practice of conducting distillation under atmospheric conditions before vacuum conditions.

Results from GC-MS analyses are summarized in Figures 2−4 for the six bio-oil types. Figures S1−S3 of the Supporting Information show the chromatograms for the TGRP bio-oil distillates. For all distillations, fraction 1 consisted almost entirely of acetone due to residual acetone from the filtration procedure. In order to compare equally among bio-oil types, GC-MS results from specific fractions within each run were mathematically combined by weighted averaging, which normalized the number of fractions. All regular bio-oil distillations show three fractions after this procedure. Figures 2−4 do not include furfural in the analyses because the compound is found only in regular bio-oil. As observed in part b of Figures 2−4, regular bio-oil distillates only consisted of acetic acid and phenols. Due to the significant increase in component purities, total weight percents of compounds observable by GC-MS increased from <20% to beyond 60−

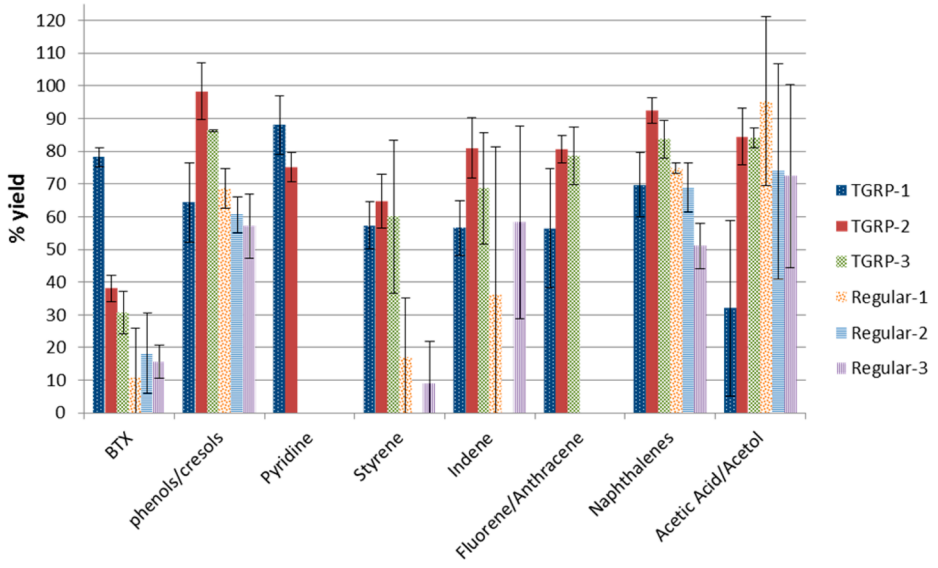


**Figure 5.** Overall yields of each compound type from the distillation process.

70%. The latter percentages only account for specific compounds for which we created GC-MS standards and calibration curves.

With the exception of Type 1 bio-oil, mathematically combined fractions from all recycle bio-oil distillations show six fractions. Type 1 bio-oil only produced five fractions total, primarily due to the relatively narrow product distribution (i.e., very high fraction of naphthalenes in Table 1), which caused a smaller variety in $T_{ov}$ observed. This phenomenon can be observed in Figure 2a. The last two fractions contain high concentrations of naphthalenes. Because naphthalenes exist as solids at room temperature, their distillation required supplemental heating of the condenser to facilitate flow. Subsequently, the final two fractions in Figure 1 exist primarily as solids (inset, Figure S1, Supporting Information). In Figure 2a, fraction 2 (60−125 °C), Type 1 oil distillate contained the only significant concentrations of pyridine recovered (∼10%) and the greatest concentration of recovered indenes.

With regard to Type 2, Figure 3 illustrates the recovery of phenols throughout the fractions in varying concentrations. This can be attributed to the high concentration of phenolics originally present in the bio-oil (Table 1). Subsequently, the fractions from Type 2 oil contain phenols in the highest concentrations (35−45%). Type 3 bio-oil distillation fractions (Figure 4) contained greater concentrations of acetic acid persistently, even at temperatures above the acetic acid boiling point. As a result, greater losses are attributable to the reactions of phenols at said temperatures under acidic conditions. Although Type 3 had one fraction with a higher phenol concentration (40−45%), this only existed in one fraction, in contrast to the persistent abundance of phenols from Type 2 oil distillation. Generally speaking, all TGRP bio-oil distillations followed identical patterns, with respect to boiling point sequences: BTX (benzene, toluene, xylenes), followed by styrene, indene, phenols, naphthalenes, and fluorene/anthracene. Each component had the smallest error bar (least variation in concentration between trials) when closest to the actual component boiling point.

**Overall and Component Yields.** Fractional compositions by themselves do not reveal complete information on any potential product losses from the distillation process. Thus, we calculated the overall yields of individual components post-distillation (Figure 5), as compared to the composition before bio-oil filtration. Figure 5 takes into account the total mass yields across all fractions per experiment. Yields of BTX compounds were generally lower due to losses from the acetone filtration and evaporation step. Compounds found only in TGRP bio-oils include styrene, pyridine, sometimes indene, and fluorene/anthracene. Larger error bars exist for styrene and indene yields, primarily due to the polymerizable nature of these molecules. Generally, distillation of all compounds produced greater yields for TGRP bio-oils than regular pyrolysis bio-oil, except for acetic acid/acetone. For regular bio-oils, distillation always produced acetic acid yields greater than 100%, accompanied by small acetol yields (≪ 50%). The greater than 100% recovery of acetic acid indicates that reactions producing acetic acid occur during heating (e.g., hydrolysis of acetate esters present in the bio-oil). Moderate yields of acetic acid from TGRP bio-oils also correlate with the low acid content due to the lower rate of polymerization/side reactions. Acetol loss is likely due to its reaction with other components in the sample. Because acetol is bifunctional (alcohol and ketone), it can act as a cross-linker, resulting in the formation of higher molecular weight species that contribute toward the nondistillable bottoms. Only Types 1 and 2 bio-oils yielded pyridine. We recovered phenols and naphthalenes in relatively high yields across all oils, although the greatest yields came from TGRP bio-oils. Phenols and naphthalenes generally boil in the middle range experimentally, so they are not affected by prevolatilization product losses or entraptment within the solid bottoms product.

While providing useful information, the percent yield analysis by itself does not accurately describe the amount of useful products produced. Distillation can recover a valuable compound at high yields, even if the compound comprises an insignificant fraction in the bio-oil. Hence, we weighed all samples as part of an overall mass balance. We also performed the Karl Fischer analysis on bio-oils and distillates in order to account for mass occupied by moisture. The KF results also aid in measuring any possible production of water from undesired reactions. Condensation reactions between alcohols and free acids or carbonyls occur producing water.[22] Figure 6

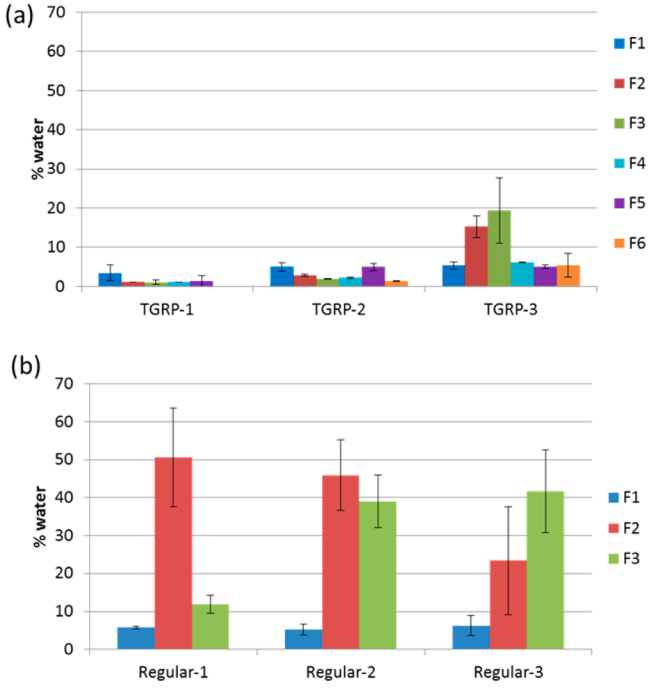


**Figure 6.** Moisture content of distilled fractions from (a) TGRP and (b) regular bio-oils. Larger steadier increases in moisture are observed in regular bio-oils, indicating more condensation reactions and loss of product.

summarizes the Karl Fischer analysis on bio-oil distillates. For all TGRP bio-oil distillates, moisture contents generally remain at or below 5%, except for Type 3, wherein percentages near 15% and 20% are observed for two fractions. Even with only three fractions to observe, the regular bio-oil fractions always exhibit high percentages of water (30−60%) after the initial acetone fraction. The differences in actual yields between TGRP and regular bio-oils greatly exceed what is expected. Hence, distillation can recover valuable compounds from TGRP bio-oils in much greater and profitable amounts.

One important observation pertains to the presence of water throughout the entire distillation. TGRP oil distillate fractions all contain some water, even when $T_{ov}$ greatly exceeds the boiling point of water (>200 °C under vacuum, compared with 100 °C atmospheric pressure). Hence, condensation-type reactions occur throughout the distillation process at various temperatures. However, the maximum activity for condensation reaction appears between 100−115 °C, and this is evidenced by the increase in water production for TGRP-3 and regular bio-oil distillations. The water appearing at 100 °C is likely from the original water content plus condensation reactions. Also observable is another small spike in water production (albeit a small spike) in the fifth fractions of Types 1 and 2 TGRP and the sixth fraction of TGRP-3, which corresponds to 185−200 °C. Phenol is known to form an azeotrope with water, so in such a complex mixture of compounds, some water can remain at this temperature. It is also possible that the breakdown of high molecular weight esters occurs at this temperature.

Alongside Karl Fischer moisture measurements, the actual mass balance yields (Table 2) complete the picture with regards to process efficiency. The top section of Table 2 displays the percentage yields that the starting bio-oil contributes to each fraction. For example, fraction 2 from Type 2 TGRP oil comprises 8.0% of the starting bio-oil by mass. Percentages

**Table 2. Fractional Yields, with Respect to Starting Bio-Oil[a]**

| | TGRP | | | regular | | |
|---|---|---|---|---|---|---|
| % yield from bio-oil | Type 1 | Type 2 | Type 3 | Type 1 | Type 2 | Type 3 |
| F1 | – | – | – | – | – | – |
| F2 | 3.9 | 8.0 | 5.2 | 14.2 | 29.2 | 33.3 |
| F3 | 7.4 | 8.0 | 6.3 | 10.0 | 3.9 | 5.6 |
| F4 | 7.7 | 12.5 | 8.6 | | | |
| F5 | 37.4 | 9.8 | 6.7 | | | |
| F6 | | 17.6 | 23.4 | | | |
| water yield % | 63.0 | 55.6 | 198.7 | 93.7 | 166.8 | 183.3 |
| oil yield (dry) | 56.2 | 55.8 | 50.2 | 16.5 | 19.3 | 28.2 |
| overall yield | 56.3 | 55.8 | 54.1 | 24.2 | 33.1 | 38.9 |

[a]The first fraction was not counted because it consisted nearly 100% of residual acetone from filtration. Regular bio-oils only produced three fractions, and Type 1 TGRP bio-oil produced only five fractions.

were used in order to normalize equally among runs with different starting amounts. The bottom section of Table 2 displays yields of (1) water, (2) organic (dry basis), and (3) overall liquid yield from distillation. One can immediately see the differences in how fractional yields are distributed. The overall mass balance closure of the distillation process averaged 70−80%. The drop in distillation mass balance closure is primarily due to the difficulty in removing and collecting bottoms residual solids because the residuals are very hard and adhere strongly to the flask. Taking this into consideration, the residual solids make up 14−20% of the TGRP-1 and TGRP-2 distillates and 30−40% of the remaining distillates. There are also possible losses of distillates due to volatility and/or entrapment in the column and/or condenser.

For Type 1 TGRP and regular oils, the largest amount of recovered organics comes from the vacuum distillation fraction (>37%). This phenomenon is also observed in the Type 3 regular bio-oil. Type 1 oils gave an average organic yield of 56%, although larger organic yields were obtained (65%). Hence, while Type 1 bio-oils exhibit promising yields, a potentially scaled-up process may require greater costs than Types 2 or 3, either due to the capital costs of vacuum distillation or the operational costs of higher boiling temperatures. Out of all six oils, Type 2 oils provided the greatest distillate mass under atmospheric conditions (nearly 40%) and the smallest water yield. Both Type 2 TGRP and regular oils yielded the least amount under vacuum by mass, as compared to other TGRP and regular bio-oils.

For some processes, distillation produced >100% water yield, indicative of excessive oligomerization by condensation reaction. While Type 3 is the only TGRP bio-oil with greater than 100% water yield, the dry organic yield remained similar in magnitude to the other TGRP bio-oils. This difference in behavior of Type 3 oil comes from the higher ratio of alcohol:acid content, which results in less depletion of distillable organics by the acid. Regular bio-oil distillation always produced much smaller yields of dry organics. Regardless of water yields, TGRP oils show superiority over regular oils due to the amount of dry organics obtained. On top of low yields, most of the organics from regular bio-oil comprise of acetic acid. Furthermore, the bio-oil produced with the optimal tail-gas recycle rate (70%) is the most optimal bio-oil for distillation, as evidenced by the drop in efficiency for 50% TGRP-Type 3. In essence, both the dry organic yield and the acid content correlate well with the tail-gas recycle rate.


dx.doi.org/10.1021/sc5002879 | ACS Sustainable Chem. Eng. 2014, 2, 2042−2052

**Elemental and TAN Analysis of Distillates.** Because distillation can separate TGRP bio-oils into chemical families (phenols, hydrocarbons, etc.), the potential exists for distillation to act as an intermediate upgrading step. To evaluate upgradability, we performed elemental analysis on TGRP bio-oils and their distillate fractions. Figure 7a–c shows Van Krevelen diagrams of the distillate fractions, grouped according to bio-oil types. Van Krevelen diagrams assist in mapping out product compositions, with respect to the desired end product (e.g., gasoline). Each plot consists of results from duplicate distillation experiments, and each coordinate represents one fraction. All three bio-oils show a distinct separation of a high O:C ratio undesired product (region 1), indicative of high acids content. Most of the coordinates fall in an area more conducive to better fuel properties (region 2). Specifically, Type 2 distillate coordinates (Figure 7b) appear vertically higher from the original bio-oil coordinate, indicating that distillation of Type 2 oils provides a net effect of hydrogenation (i.e., higher H:C ratio). On the other hand, Types 1 and 3 distillate coordinates (Figure 7a and c) provide distillates that appear directly to the left of the original bio-oil coordinate, indicative of a net deoxygenation effect. In order to approach gasoline-grade fractions, hydrogenation with external hydrogen is required. Regardless, the distinct regions illustrate how $T_{ov}$ can guide batch distillation toward predictable outcomes.

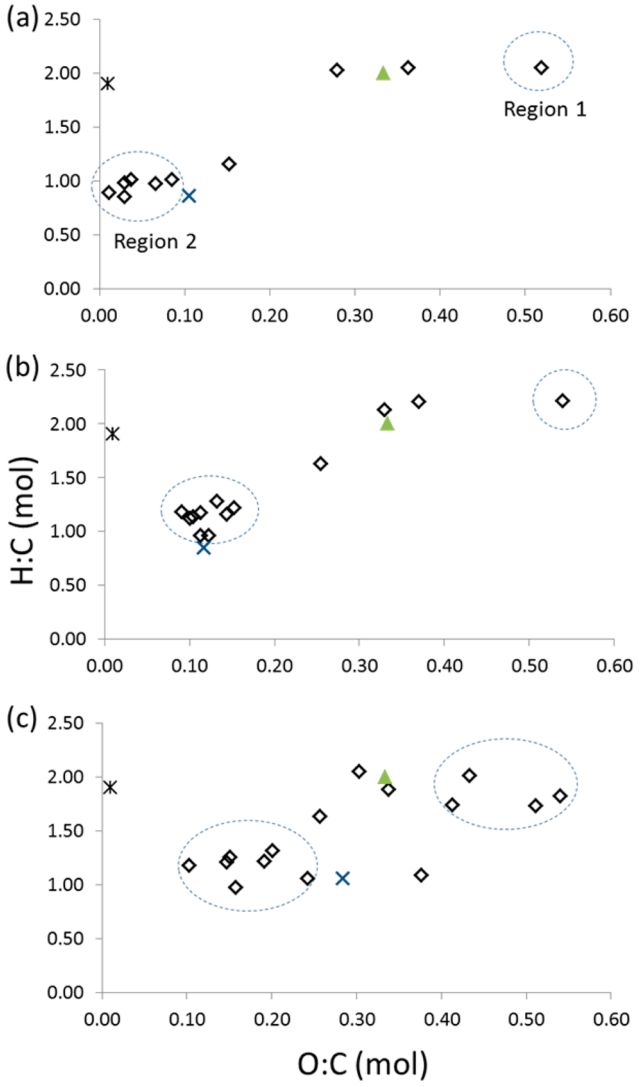


**Figure 7.** Van Krevelen diagrams of distilled recycle bio-oil fractions from (a) Type 1, (b) Type 2, and (c) Type 3 TGRP bio-oils. Plots include fractions from duplicate experiments. Coordinates are represented as follows: distillates (◇), bio-oil (×), acetone (△), and gasoline (∗).

With regards to TAN measurements (Table 3), Types 2 and 3 fractions each contribute a singular fraction with excessively high TAN (>300 mg KOH/g). In each distillation run, this peak TAN value correlates with the fraction containing the highest concentration of acetic acid, each between 10–50 wt %. Type 1 did not contain any acetic acid to start, which prevented the aforementioned behavior, that is, all TAN values were less than 53. Hence, the TAN values show the effectiveness of isolating acetic acid from more valuable compounds. Type 3 persisted in acidity after its initial peak value, which can explain the lack of upgradability in some of the coordinates. As with other variables discussed previously, the deviation from optimal alcohol:acid ratio for Type 3 oils relates to this effect. Isolation of acetic acid into one distillate fraction (e.g., Figure 3a at 155 °C) allows the remaining TGRP bio-oil distillates to be free of acid instabilities. Subsequently, a pyrolysis biorefinery could potentially produce acetic acid and purified commodity chemicals in parallel.

**Table 3. Total Acid Numbers (mg KOH/g) of Distillate Fractions for TGRP Bio-Oils**

| | Type 1 | Type 2 | Type 3 |
|---|---|---|---|
| F1 | – | – | – |
| F2 | 44.4 | 345.6 | 54.9 |
| F3 | 22.6 | 29.1 | 479.7 |
| F4 | 13.5 | 29.1 | 112.8 |
| F5 | 5.3 | 55.4 | 68.7 |
| F6 | | 11.1 | 55.1 |
| TGRP bio-oil | 17.70 | 23.73 | 40.89 |

**Naphthalene Isolation.** Because distillation has effectively concentrated valuable compounds into high concentrations (30–70%), one could take these fractions and further purify them through simpler means. The best opportunity for this came about with the solid-phase distillates of Type 1 TGRP oil. GC-MS indicated that the solid was very predominantly naphthalene, with small amounts of similar derivatives. Hence, we recrystallized the crude solid in methanol, because methanol dissolves hydrocarbons at high temperatures but not at low temperatures. Figure 8 shows the purified solid naphthalene and its associated spectra. GC-MS (Figure 8b) indicated only <5% anthracene and ∼1% methylnaphthalene, with the balance naphthalene. The purity of the naphthalene was also verified by $^{1}H$ and $^{13}C$ NMR with anthracene as the only detectable impurity (Figure 8).

**Computation of Distillation Curves.** The ambiguity of regular bio-oil compositions has continually hindered precise process modeling. The results in Table 1 and Figures 2–4 provide valuable information for process modeling purposes and warrants investigation. TGRP oil distillate compounds emanate from the oil itself. In contrast, regular bio-oil distillate compounds arise as products from undesired side reactions. Hence, our first assumption is that all volatile components from TGRP oils can be modeled as a simple nonreactive mixture. Due to the nonreactivity assumption, along with the fact that bottoms products remain undistilled, bottoms products and/or


dx.doi.org/10.1021/sc5002879 | ACS Sustainable Chem. Eng. 2014, 2, 2042–2052

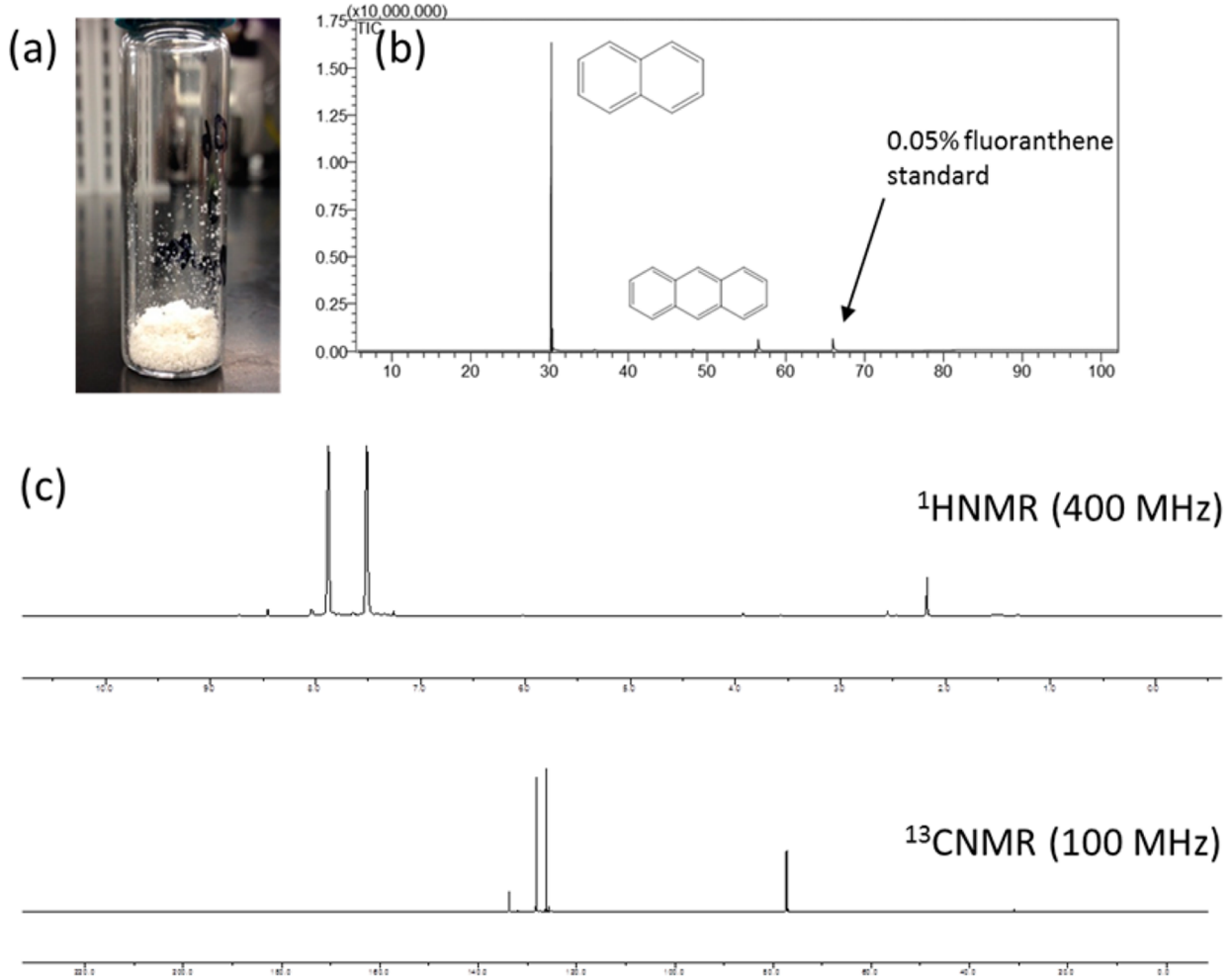


**Figure 8.** (a) Solid naphthalene recrystallized from fractions of distilled TGRP oil (Type 1). Characterization by GC-MS (b) and NMR ($CDCl_3$) (c) show the solid to be 95% pure, with the balance comprised anthracene.

high molecular weight lignins are assumed to play negligible roles in TGRP oil distillation profiles. Because nondistilled bottoms remain isolated from a modeling standpoint, the bio-oil GC-MS measurements play a much stronger role in determining feed composition. Although we cannot measure or determine every volatile component, we measured the large majority of them. The unmeasured components are simple derivatives that do not differ significantly from a chemical property standpoint (e.g., dimethyl phenol vs cresol have similar intermolecular forces). Hence, our third assumption is that the bio-oil GC-MS compositions are representative of the bio-oil volatiles as a whole (while disregarding nonvolatile bottoms).

We entered the GC-MS compositions of each TGRP bio-oil type into Pro-II as a user-defined mixture (Table S3, Supporting Information); we scaled the GC-MS compositions such that they totaled 100%. Although many of the TGRP oil chemical components from Table 1 have similar boiling points, their thermodynamic interactions as mixtures determine their volatilities. The Pro-II simulation software computed theoretical distillation curves based on solution equilibrium activity models. These computed curves are plotted in Figure 9 (∗ with dashed lines), along with the corresponding experimental data (dots). For experimental data points, the cumulative percent distilled was based on the total mass of distillates, which more accurately correlates with the Pro-II model. We used $T_{ov}$ to plot data points accordingly. Temperature values recorded during vacuum distillation were translated to an equivalent atmospheric temperature using a nomograph (Sigma-Aldrich Web site). To ensure accuracy, the actual experimental fractions were used instead of the mathematically combined fractions from Figures 2−4. For Type 1 and 2 TGRP oils, experimental data correlated very well with the theoretical model. Particularly with Type 2 oils, the model maintains accuracy even during the steep increase between 175 and 200 °C. For Type 3 oils, the model accuracy begins to break down, likely from inconsistent results due to side reactions. Hence, while useful chemicals are obtainable at reasonable yields for Type 3, integration of Type 3 oils into a refinery may not progress as smoothly due to model fluctuations (and hence scale-up fluctuations). Accuracy improvement could come about by modeling the side reactions that were discussed previously. It is worth noting that the accuracy of Type 2 distillation modeling correlates with Type 2 as yielding the greatest recovery under atmospheric distillation. Nonetheless, this model serves as the first known process model link between pyrolysis bio-oil and real chemicals. Furthermore, TGRP oil distillation attains the product quality sought out by catalytic fast pyrolysis without any need or cost of catalyst.

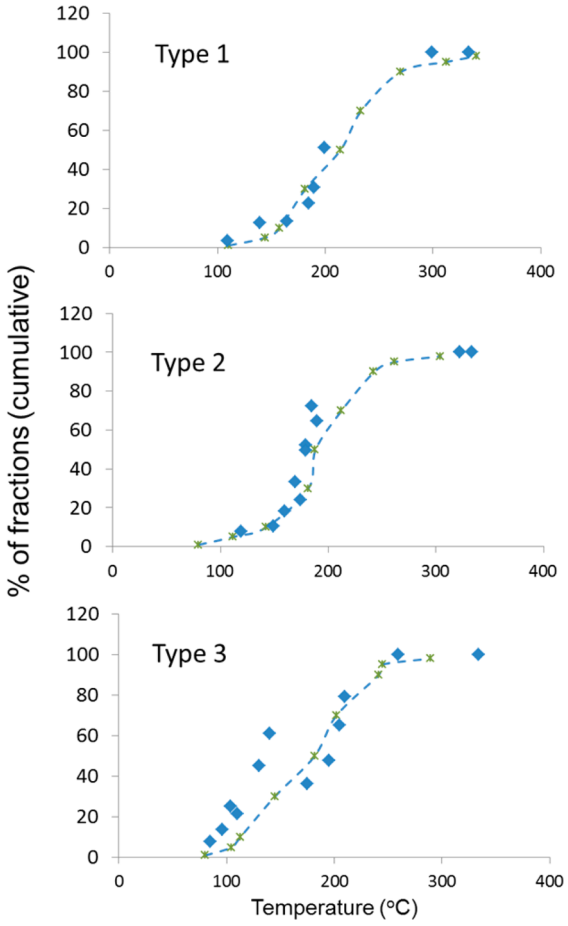


**Figure 9.** Distillation curves of the three TGRP bio-oils based on experiment (◇) and theoretical computation (∗ with dashed line). Temperatures recorded under vacuum distillation were converted to their atmospheric pressure equivalents.

## CONCLUSIONS

We used a continuous fast pyrolysis process to produce bio-oils of widely varying chemical identities, created by recycling the noncondensable tail-gas as a fluidizing and reactive atmosphere (TGRP). We demonstrated the efficient distillation of TGRP oils into valuable commodity chemicals at high yields. As compared with regular bio-oil, TGRP oil distillation produced more than three times the yield of organics. Distillation of TGRP oils also produced more than 10 times the amount of desirable components (BTX, naphthalenes, etc.) after subtraction of less desired recoverables (e.g., acetic acid). Type 1 TGRP oil, which was rich in naphthalenes, produced the cleanest distillates with the greatest yields, although a large majority of the yield requires vacuum distillation and/or higher temperatures. These properties of Type 1 oil owe to the narrow product distribution of bicyclic aromatics. Type 2 bio-oil yielded the most oil under atmospheric distillation, and its distillates contained the most phenols. Type 3 oil yielded high amounts of organics post-distillation relative to regular bio-oil, but higher concentrations of acids due to the lower recycle rate used during production reduced the dry organic yield and increased the water yield. The greater acid concentration induces product loss via condensation polymerization, even at temperatures above the acetic acid boiling point. Elemental and TAN analyses of distillates confirm the trends obtained by GC-MS. Types 1 and 3 TGRP distillates are oxygen-deficient compared with their respective bio-oils, while Type 2 distillates are relatively hydrogen-enriched. We also purified a single component (naphthalene) in significant amounts. Theoretically calculated distillation curves for Types 1 and 2 bio-oils matched well with experimentally derived curves. The isolated products and computational models obtained from TGRP bio-oil distillation could significantly improve pyrolysis biorefinery economics. Most importantly, TGRP oils can potentially integrate directly into a refinery prehydrotreatment.

## ASSOCIATED CONTENT

### Supporting Information

Information on process mass balances, GC-MS chromatograms, and Pro-II simulation inputs. This material is available free of charge via the Internet at http://pubs.acs.org.

## AUTHOR INFORMATION

### Corresponding Author

*Phone: 215-836-3797. Fax: 215-233-6406. E-mail: yaseen.elkasabi@ars.usda.gov.

### Notes

The authors declare no competing financial interest.

Mention of trade names or commercial products in this publication is solely for the purpose of providing specific information and does not imply recommendation or endorsement by the U.S. Department of Agriculture. USDA is an equal opportunity provider and employer.

## ACKNOWLEDGMENTS

We acknowledge Christina Papadimitriou (summer 2013 USDA Pathway scholar from the University of South Carolina) and Kevin Minsker (Drexel University co-op, Fall 2013), who each provided support work for the distillation and characterization experiments. We also acknowledge Craig Einfeldt, who provided support work for the fast pyrolysis experiments, and Anna Pighinelli who provided the eucalyptus bio-oil. The USDA-NIFA-BRDI Grant 2012-10008-20271 is hereby acknowledged.

## REFERENCES

(1) Bridgewater, A. V. Review of fast pyrolysis of biomass and product upgrading. *Biomass Bioenergy* **2012**, *38*, 68−94.

(2) Talmadge, M. S.; Baldwin, R. M.; Biddy, M. J.; McCormick, R. L.; Beckham, G. T.; Ferguson, G. A.; Czernik, S.; Magrini-Bair, K. A.; Foust, T. D.; Metelski, P. D.; Hetrick, C.; Nimlos, M. R. A perspective on oxygenated species in the refinery integration of pyrolysis oil. *Green Chem.* **2014**, *16*, 407−453.

(3) Speight, J. G. In *The Chemistry and Technology of Petroleum* , 3rd ed.; Marcel Dekker: New York, 1999; pp 215−216.

(4) Jana, A. K. Heat integrated distillation operation. *Appl. Ener.* **2010**, *87*, 1477−1494.

(5) Schultz, M. A.; Stewart, D. G.; Harris, J. M.; Rosenblum, S. P.; Shakur, M. S.; O'Brien, D. E. Reduce Costs with Dividing-Wall Columns. *Chemical Engineereing Practice Magazine*, May **2002**, 64−71.

(6) Kolbe, B.; Wenzel, S. Novel distillation concepts using one-shell columns. *Chem. Eng. Proc.* **2004**, *43*, 339−346.

(7) Srivastava, V. C. An evaluation of desulfurization technologies for sulfur removal from liquid fuels. *RSC Adv.* **2012**, *2*, 759−783.

(8) Ali, M. F.; Abbas, S. A review of methods for the demetallization of residual fuel oils. *Fuel Proc. Technol.* **2006**, *87*, 573−584.

(9) Elliott, D. C. Historical developments in hydroprocessing bio-oils. *Energy Fuels* **2007**, *21*, 1792−1815.

(10) Zacher, A. H.; Olarte, M. V.; Santosa, D. M.; Elliott, D. C.; Jones, S. B. A review and perspective of recent bio-oil hydrotreating research. *Green Chem.* **2014**, *16*, 491−515.
(11) Dobele, G.; Dizhbite, T.; Urbanovich, I.; Andersone, A.; Ponomarenko, J.; Telysheva, G. Pyrolytic oil on the basis of wood and the antioxidant properties of its water-soluble and -insoluble fraction. *J. Anal. Appl. Py.* **2009**, *85*, 81−86.
(12) Oasmaa, A.; Kuoppala, E. Solvent fractionation method with brix for rapid characterization of wood fast pyrolysis liquids. *Energy Fuels* **2008**, *22*, 4245−4248.
(13) Meier, D.; van de Beld, B.; Bridgewater, A. V.; Elliott, D. C.; Oasmaa, A.; Preto, F. State-of-the-art of fast pyrolysis in IEA bioenergy member countries. *Renewable Sustainable Energy Rev.* **2013**, *20*, 619−641.
(14) KiOR. http://www.kior.com (accessed 2013).
(15) Friedman, G. H. *Follow-Up Audit of the Department of Energy's Financial Assistance for Integrated Biorefinery Projects*; DOE/IG-0893; Washington, DC, 2013.
(16) Capunitan, J. A.; Capareda, S. C. Characterization and separation of corn stover bio-oil by fractional distillation. *Fuel* **2013**, *112*, 60−73.
(17) Mahfud, F. H.; Melin-Cabrera, I.; Manurung, R.; Heeres, H. J. Biomass to fuels: Upgrading of flash pyrolysis oil by reactive distillation using high boiling alcohol and acid catalysts. *Process Saf. Environ. Prot.* **2007**, *85*, 466−472.
(18) Wang, C.; Hu, Y.; Chen, Q.; Lv, C.; Jia, S. Bio-oil upgrading by reactive distillation using p-toluene sulfonic acid catalyst loaded on biomass activated carbon. *Biomass Bioenergy* **2013**, *56*, 405−411.
(19) Frey, S. J.; Marinangeli, R. E.; Brandvold, T. A.; Koch, M. B.; Abrahamian, V. B.; Noga, J. M.; Traynor, T. J. Low metal, Low Water Biomass-Derived Pyrolysis Oils and Methods for Producing the Same. U.S. Patent 2011/0146141 A1, 2011.
(20) Wang, S. W.; Gu, Y.; Liu, Q.; Yao, Y.; Guo, Z.; Luo, Z.; Cen, K. Separation of bio-oil by molecular distillation. *Fuel Proc. Technol.* **2009**, *90*, 738−745.
(21) Guo, X.; Wang, S.; Guo, Z.; Liu, Q.; Luo, Z.; Cen, K. Pyrolysis characteristics of bio-oil fractions separated by molecular distillation. *Appl. Energy* **2010**, *87*, 2892−2898.
(22) Zhang, X. S.; Yang, G. X.; Jiang, H.; Liu, W. J.; Ding, H. S. Mass production of chemicals from biomass-derived oil by directly atmospheric distillation coupled with co-pyrolysis. *Sci. Rep.* **2013**, *3*, 1120 DOI: 10.1038/srep01120.
(23) Agblevor, F. A.; Mante, O.; Abdoulmoumine, N.; McClung, R. Production of stable biomass pyrolysis oils using fractional catalytic pyrolysis. *Energy Fuels* **2010**, *24*, 4087−4089.
(24) Mullen, C. A.; Boateng, A. A.; Goldberg, N. M. Production of deoxygenated biomass fast pyrolysis oils via product gas recycling. *Energy Fuels* **2013**, *27*, 3867−3874.
(25) Boateng, A. A.; Daugaard, D. E.; Goldberg, N. M.; Hicks, K. B. Bench-scale fluidized-bed pyrolysis of switchgrass for bio-oil production. *Ind. Eng. Chem. Res.* **2007**, *46*, 1891−1897.
(26) Pighinelli, A. L. M. T.; Boateng, A. A.; Mullen, C. A.; Elkasabi, Y. Evaluation of Brazilian biomasses as potential feedstocks for fuel production via fast pyrolysis. *Energy Sustainable Dev.* **2014**, *21*, 42−50.